

Original Article

A novel hybrid 3D-printed titanium scaffold for osteogenesis in a rabbit calvarial defect model

Bo Yin¹, Bingjian Xue¹, Zhihong Wu^{2,3}, Jiguang Ma¹, Keming Wang¹

¹Plastic Surgery Hospital, Chinese Academy of Medical Sciences and Peking Union Medical College, No. 33, Badachu Road, Shijingshan District, Beijing 100144, China; ²Central Laboratory, Peking Union Medical College Hospital, Peking Union Medical College and Chinese Academy of Medical Sciences, No. 1 Shuaifuyuan, Beijing 100730, China; ³Beijing Key Laboratory for Genetic Research of Bone and Joint Disease, No. 1 Shuaifuyuan, Beijing 100730, China

Received August 20, 2017; Accepted December 24, 2017; Epub February 15, 2018; Published February 28, 2018

Abstract: The aim of this study was to explore an innovative method to improve the osteogenic ability of porous titanium. We used gelatin (Gel) and nano-hydroxyapatite (nHA) to construct micro-scaffolds within the pores of porous titanium alloy. We compared three groups: control, Gel:nHA = 1:0, and Gel:nHA = 1:1. We assessed cell attachment, cell proliferation, and osteogenic (alkaline phosphatase [ALP] and collagen type 1 [Col-1]) and cytoskeletal (Talin) gene and protein expression in MC3T3-E1 cells. We also evaluated osteogenic abilities in a rabbit calvarial defect model. Our results showed that micro-scaffolds can improve new bone formation both in vitro and in vivo. Between the two micro-scaffold groups, the Gel:nHA = 1:1 group exhibited the most satisfactory results. It had a multi-hierarchical pore structure with a mean pore size of $156\pm 86\ \mu\text{m}$. The Gel:nHA = 1:1 group exhibited significantly higher gene and protein expression of ALP, Col-1, and Talin. This group also exhibited the most new bone volume during in vivo experiments. The 3D micro-scaffold structure was an effective method of porous titanium modification that not only provided appropriate cell growth conditions but may also be used as a carrier of bioactive factors in the future.

Keywords: 3D-printed scaffold, Ti6Al4V, bone regeneration, osteogenesis

Introduction

The treatment of bone defects has always been a difficult problem. Bone defects with a length 1.6 times greater than their diameter require bone grafts [1, 2]. Both autografts and allografts have limitations, such as the risk of infection, donor site pain, and immune rejection [3, 4]. Natural or synthetic biological materials, such as polylactic acid, polylactic-co-glycolic acid, and tricalcium phosphate, have good biocompatibility and degradation performance; however, overcoming their insufficient strength and controlling their degradation time window have remained a challenge [5-7].

Titanium alloy has been used in dentistry and orthopedic surgery for many years because of its safety and excellent mechanical properties. The advent of 3-dimensional (3D) printing techniques provided new potential applications for titanium alloy, allowing the production of

high-precision, personalized, porous connected structures as good bone defect substitutes to meet clinical needs. However, titanium is bio-inert, so it cannot promote bone regeneration [8]. In previous reports, the pore size recommended for cell growth into a scaffold was approximately 100-300 μm [9]. With scaffolds for bone tissue engineering, the aim is to minimize metal volume and maximize bone volume; a pore size that is too small increases the proportion of metal. Recent studies of porous titanium have generally used a pore size of 500-1500 μm . Research into porous titanium modifications has mainly focused on small pore sizes, from a 2-dimensional (2D) perspective [10-13].

In the experiments described in this report, we prepared porous titanium with a pore size of 1500 μm , under the premise that it will provide sufficient mechanical strength, and proposed the concept of 3D modification. We then

Hybrid titanium scaffold for osteogenesis

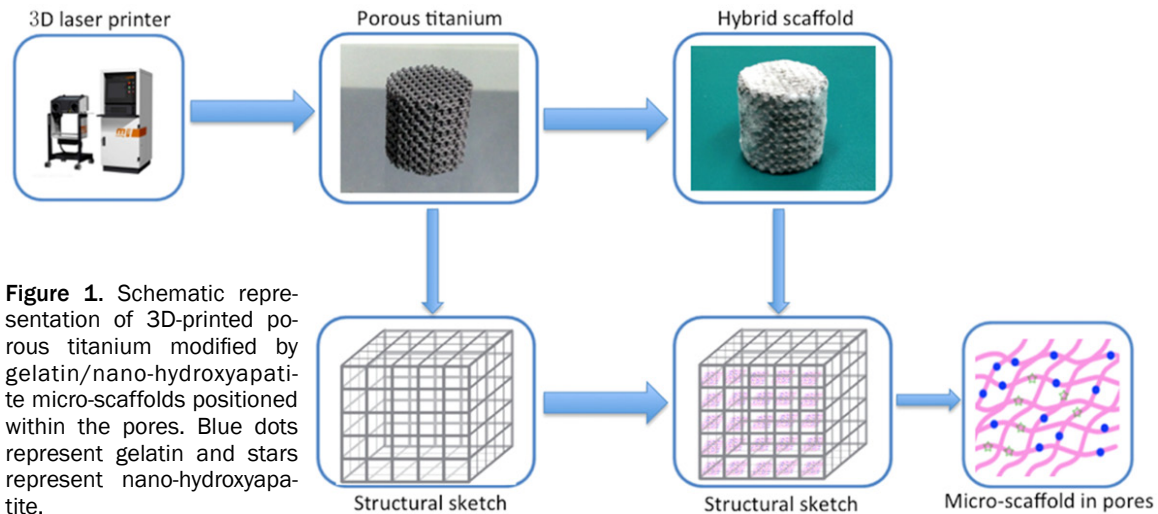


Figure 1. Schematic representation of 3D-printed porous titanium modified by gelatin/nano-hydroxyapatite micro-scaffolds positioned within the pores. Blue dots represent gelatin and stars represent nano-hydroxyapatite.

created degradable micro-scaffolds with a 3D structure positioned without the titanium pores to accelerate osteogenesis. The micro-scaffolds were made of gelatin and nano-hydroxyapatite (nHA). As collagen and HA are the most important kinds of bone matrix, they have good bone induction and bone conduction capacity [14, 15]. Gelatin is a denatured form of collagen that contains many functional amino acids and has almost identical composition to that of collagen, so it is suitable for bone tissue applications. nHA can enhance new bone formation by increasing osteoblast adhesion, proliferation, osteointegration, and calcium deposition [16]. Thus, in our hybrid scaffold system, porous titanium provides mechanical strength, whereas Gel/nHA micro-scaffolds provide a micro-environment similar to that of normal bone to promote cell proliferation and differentiation.

In this study, we evaluated the effects of our hybrid scaffold system on cell attachment, cell proliferation, and osteogenic and cytoskeletal gene and protein expression *in vitro*. We also examined its osteogenic abilities in a rabbit calvarial defect model.

Materials and methods

Porous titanium fabrication

We used selective laser melting (Concept Laser, Germany) to fabricate porous titanium scaffold from spherical Ti6Al4V powder (American Society for Testing and Materials B348, grade 23) (Figure 1). Based on computer-aided

design data for porous structures, a dodecahedron was designed as the unit cell with the following characteristics: strut size = 300 μm , pore size = 1500 μm , and porosity = 84.8%. The specimens were disk-shaped samples: $\varnothing = 5\text{ mm}$ and $\varnothing = 30\text{ mm}$ for *in vitro* assays (Figure 2A and 2D), and $\varnothing = 8\text{ mm}$ for animal experiments. All samples underwent post-production heat treatment and were cleaned in an ultrasonic bath to remove residual titanium particles and impurities.

Porous titanium modified by gelatin/nano-hydroxyapatite (Gel/nHA) 3D micro-scaffolds

Gel/nHA micro-scaffolds were prepared by chemical crosslinking gelatin with glutaraldehyde. Briefly, for the Gel:nHA = 1:1 group, 15 mL aqueous solution of 3 wt % gelatin (type B from bovine skin; Sigma Co. Ltd, USA) and the same volume of HA (particle size = 20 nm, purity = 99%; Emperor Nano Material Co. Ltd, Nanjing, China) were ultrasonically mixed at room temperature for 3 min. After adding 0.625 wt % glutaraldehyde aqueous solution, porous titanium was placed in the solution and the solution was stirred quickly using an agitator, using centrifugal force to spread the foam into every pore of the titanium. After 12 h at 4°C to allow gelatin crosslinking, the samples were immersed two times in 0.1 mol/L aqueous glycine solution at room temperature for 1 h to block residual glutaraldehyde. This was followed by thorough washing three times with double-distilled water for 2 h using a magnetic stirring apparatus. The samples

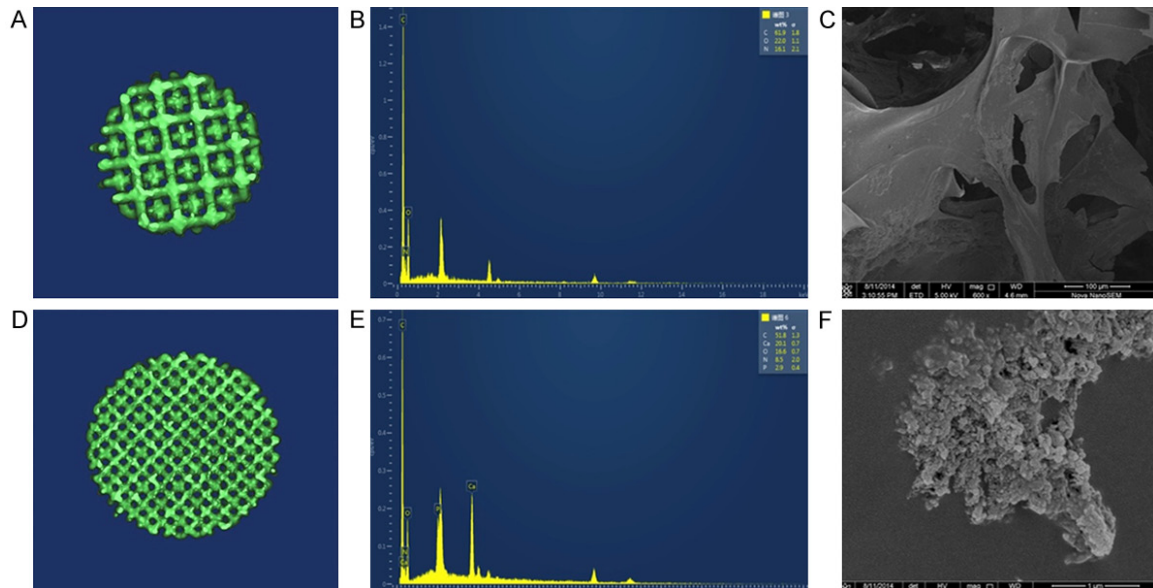


Figure 2. (A, D) Disk-shaped porous titanium specimens used for in vitro tests (A: $\varnothing = 5$ mm, D: $\varnothing = 30$ mm). (B, E) Energy dispersive x-ray spectrometry verification of the element composition of the gelatin/nano-hydroxyapatite micro-scaffolds (B: Gel:nHA = 1:0, E: Gel:nHA = 1:1). (C, F) Morphology of the micro-scaffolds in the Gel:nHA = 1:1 group, observed by scanning electron microscopy (C: 600 \times , F: 80000 \times).

were then placed at -80°C overnight and subsequently freeze-dried for 48 h. They then underwent ethylene oxide sterilization, followed by separate packaging. Morphological characteristics were observed by scanning electron microscopy (SEM; FEI, Nova NanoSEM 450) after application of gold spray. Energy dispersive X-ray spectrometry (EDS; FEI, Nova NanoSEM 450) was used to analyze the element composition of the micro-scaffolds.

Cell culture

Pre-osteoblast cells (MC3T3-E1) were purchased from the Institute of Basic Medical Sciences, Peking Union Medical College (Chinese Academy of Medical Science, Beijing, China) and cultured in α -minimum essential medium (MEM; Gibco, Grand Island, NY, USA) supplemented with 10% fetal calf serum (FCS; Invitrogen, Carlsbad, CA, USA).

Cell attachment and proliferation

Morphology of the adherent cells was examined by SEM. Briefly, a cell suspension (2.5×10^5 cells/mL, 40 μL) was placed in the scaffold in a 96-well plate and cultured for 4 h. Medium was then added, and the cells were incubated for 7 days, with the medium chang-

ed every 2-3 days. The samples were rinsed with phosphate buffered saline to remove non-adherent cells and then fixed with 2.5 wt % glutaraldehyde for 1 h. A series of gradient ethanol solutions (50%, 70%, 90%, 95%, and 100%) was used for sample dehydration, which was followed by the addition of pure isopentyl acetate. Cell morphology was observed by SEM (FEI, Nova NanoSEM 450, 10.00 kV), and samples were sputter-coated with a 10-nm thick gold film before measurements.

After the cells were cultured for 7 days, the culture medium was discarded and cell viability was assessed using the LIVE/DEAD[®] cell viability kit (Invitrogen). Fluorescence images were obtained by positive fluorescence microscopy (Nikon Eclipse 80i, Inc., Japan). Cell density was analyzed using the ImageJ software package. Six different region-of-interest fields were measured per sample ($n = 3$). The Cell Counting Kit-8 assay (CCK-8; Dojindo Molecular Technologies Inc., Minato-ku, Tokyo, Japan) was used to quantify cell proliferation after culturing the cells for 1, 3, and 7 days.

Cell differentiation

Osteogenic differentiation of attached cells was assessed by reverse transcription poly-

Hybrid titanium scaffold for osteogenesis

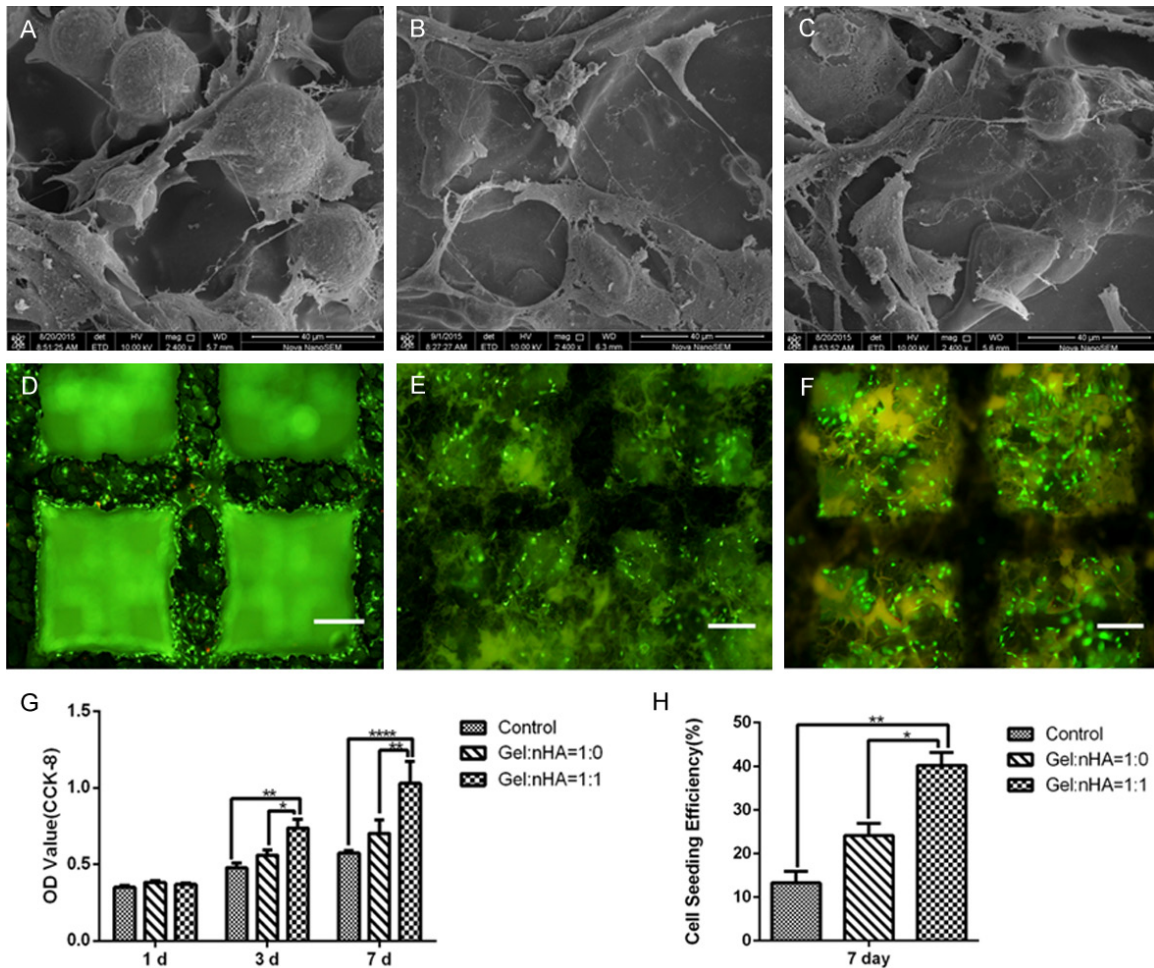


Figure 3. Cell attachment and proliferation on hybrid scaffolds. (A-C) Morphology of cells attached on the different scaffolds, as assessed by scanning electron micrography (A: control, B: Gel:nHA = 1:0, C: Gel:nHA = 1:1). (D-F) Cell seeding efficiency based on the LIVE/DEAD[®] staining viability kit (D: control, E: Gel:nHA = 1:0, F: Gel:nHA = 1:1). Scale bar: 500 μ m. (G) Cell proliferation based on optical density value of the Cell Counting Kit-8 assay. (H) Cell seeding efficiency based on LIVE/DEAD[®] staining, calculated using ImageJ software. * $P < 0.05$, ** $P < 0.01$, *** $P < 0.001$, **** $P < 0.0001$. Gel, gelatin; nHA, nano-hydroxyapatite; OD, optical density.

merase chain reaction (RT-PCR) and enzyme-linked immunosorbent assay (ELISA) at the gene and protein levels, respectively. After cells were cultured for 14 days, they were harvested ($n = 3$). Total RNA was extracted using TRIZOL reagent (Invitrogen) and reversed transcribed to cDNA using a cDNA synthesis kit (Thermo Scientific, Waltham, MA, USA). Expression levels of osteoblastic markers (alkaline phosphatase [ALP], collagen type 1 [Col-1]), and the cytoskeleton protein Talin were quantified using SYBR green master mix (KAPA Biosystems, Wilmington, MA, USA) and the StepOne Plus RT-PCR instrument (ABI, Carlsbad, CA, USA). Expression levels were calculated using the $2^{-\Delta\Delta Ct}$ method by normalizing

values to the housekeeping gene, β -actin. The following primers were used for the selected genes: ALP (forward, 5'-GGCAACTCCATCTTGGTCTG-3'; reverse, 5'-GCCTGGTAGTTGTTGTGAGCGT-3'); Col-1 (forward, 5'-ATGACCGATGATTCCCGTTC-3'; reverse, 5'-ACGCTGTTCTTG-CAGTGATAGGT-3'); and Talin (forward, 5'-TAC-TACATGCTCCGAAATGGGG-3'; reverse, 5'-CACC-GTTCCGTCTAACATCCG-3').

Commercial ELISA kits (ALP, Abcam, Cambridge, UK; Col-1, Cloud-Clone Corp, Houston, TX, USA; Talin, Cloud-Clone Corp, Houston, TX) were used to further evaluate differences in osteogenic properties among the three groups. After 14 days of culture, medium super-

Hybrid titanium scaffold for osteogenesis

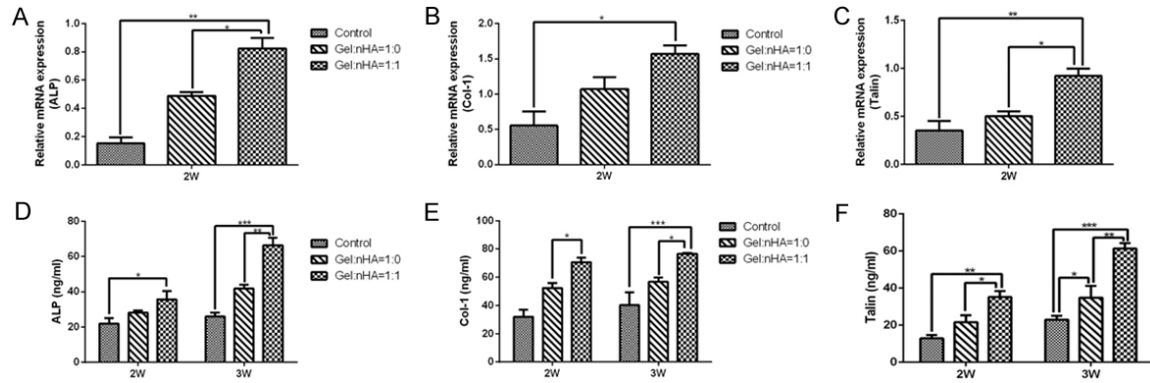


Figure 4. Osteogenic differentiation of cells seeded on scaffolds assessed by reverse transcription polymerase chain reaction (A-C) and enzyme-linked immunosorbent assay (D-F) using osteogenic (alkaline phosphatase [A, D] and collagen type 1 [B, E]) and cytoskeletal (Talin [C, F]) markers. * $P < 0.05$, ** $P < 0.01$, *** $P < 0.001$. ALP, alkaline phosphatase; Col-1, collagen type 1; Gel, gelatin; nHA, nano-hydroxyapatite.

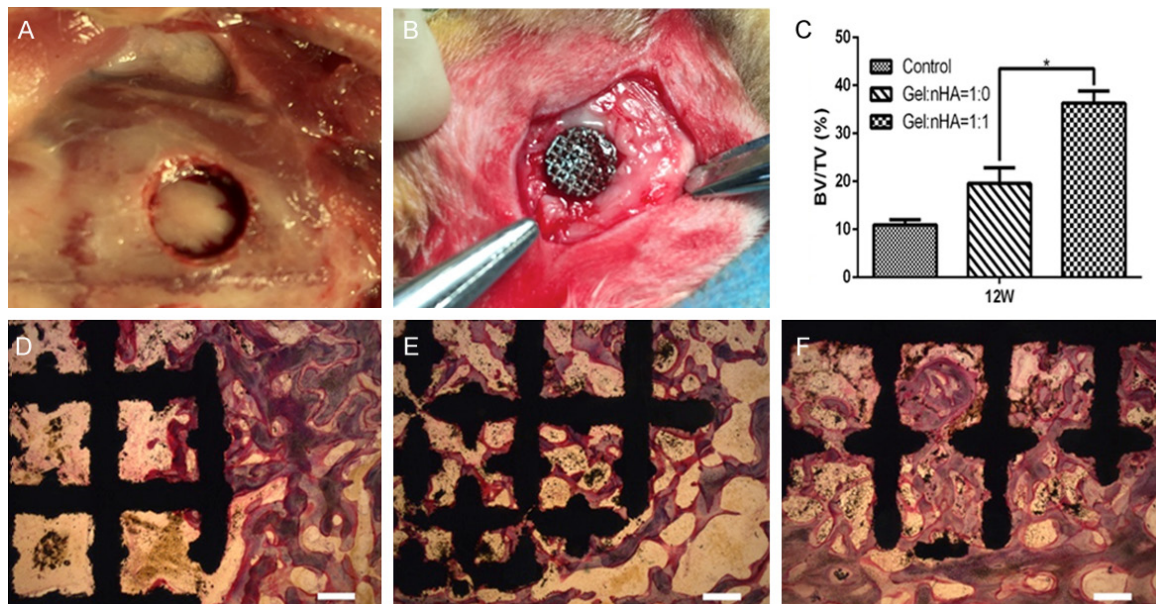


Figure 5. Surgical procedure and histological analysis of osteointegration abilities of different scaffolds. (A, B) Surgical procedure showing the scaffold implantation site (A) and an implanted scaffold (B). (C) Osteointegration at 12 weeks after surgery of the three groups represented by the bone volume/total volume (BV/TV) ratio, which was determined by ImageJ software. (D-F) Histological analysis using Giemsa-eosin staining at 12 weeks after surgery (D: control, E: Gel:nHA = 1:0, F: Gel:nHA = 1:1). Red represents new bone formation, pink represents fibrous tissue, and black represents the titanium alloy. Scale bar: 500 μm .

natants ($n = 3$) were processed according to the kit instructions, and results were calculated from a standard absorbance curve at 450 nm.

Implantation procedure

The animal care committee of Peking Union Medical College approved all animal experiments. A total of 18 healthy, skeletally-mature,

female New Zealand White rabbits (age, 20 weeks; weight, 3.4 ± 0.2 kg) were randomly divided into 3 groups (6 per group). They received porous titanium filled with nothing (control), micro-scaffolds with Gel:nHA = 1:0, or micro-scaffolds with Gel:nHA = 1:1. The rabbits were anesthetized with 10% chloral hydrate (1.2 mL/kg intravenously). An 8-mm calvarial bone defect was created using a surgical electric drill supplemented by copious 0.9% steril-

ized saline irrigation, and scaffolds were implanted press-fit into the defect without additional fixation devices (**Figure 5A** and **5B**). The incision was closed in layers and dressed with a bandage.

Histology and histomorphometric analysis

At 12 weeks after implantation, the rabbits were euthanized, and the scaffolds were removed. These specimens were dehydrated in a graded ethanol series (70% to 100%) after fixation in 10% formalin solution for 2 weeks. They were then embedded in a methylmethacrylate solution, which polymerized at 37°C within 1 week without decalcification. Samples were subsequently cut into 50- μ m transverse-section slices using a modified interlocked diamond saw (Leica Microtome, Wetzlar, Germany) and stained with Giemsa and eosin. The bone volume/total volume (BV/TV) was determined using ImageJ software package ($n = 3$).

Statistical analysis

SPSS Statistics 21.0 (SPSS, Inc., Al Monk, NY, USA) was used for the statistical analyses. Data are presented as mean \pm standard deviation. One-way analysis of variance and subsequent post hoc Tukey's test were used to investigate differences among three groups. Statistically significant was defined as a P value < 0.05 .

Results

Scaffold characterization

We successfully produced 3D-printed porous titanium (**Figures 1, 2**) with these characteristics: strut size = 352 ± 46 μ m, porosity = $80.7 \pm 4.6\%$, compressive strength = 77.4 ± 3.6 MPa, and modulus of elasticity = 3.4 ± 0.8 GPa. These are similar to the characteristics of normal human trabecular bone, which can provide adequate mechanical support without obvious stress shielding effect. We also successfully constructed the 3D micro-scaffolds within the titanium pores. SEM revealed surface features of the Gel:nHA = 1:1 group, which exhibited a multi-hierarchical structure with a mean pore size of 156 ± 86 μ m. At greater magnification, we observed the distribution of the nHA mass; the diameter was approximately 5.3 ± 3.1 μ m, which was suitable for cell attachment

and growth (**Figure 2C** and **2F**). EDS confirmed the presence of nHA in the micro-scaffolds of the Gel:nHA = 1:1 group, indicating that the hybrid scaffold had been successfully constructed (**Figure 2B** and **2E**).

Cell attachment and proliferation

Cellular morphology on the scaffolds was observed by SEM after incubation for 7 days (**Figure 3A-C**). MC3T3-E1 cells in the micro-scaffold modified groups, especially the Gel:nHA = 1:1 group, exhibited elongated and plump morphology with abundant filaments and noticeable filopodia. By contrast, cells in the control group appeared atrophic or had fewer pseudopodia and were distributed sparsely, at a low density. These results indicate that the micro-environment was beneficial for cell adhesion and proliferation in the Gel:nHA = 1:1 group. In CCK-8 assessment of cell proliferation, the Gel:nHA = 1:1 group exhibited significantly higher optical density (OD) than the other two groups at 3 and 7 days of incubation (**Figure 3G**). The cell proliferation results measured by the LIVE/DEAD® viability assay kit were consistent with the CCK-8 results (**Figure 3D-F**). Cell density calculated by ImageJ software showed that cell seeding efficiency was approximately 16% to 27% higher in the Gel:nHA = 1:1 group than in the other two groups (**Figure 3H**).

Osteogenic differentiation

Osteogenic differentiation capability was detected by RT-PCR at 14 days of incubation (**Figure 4**). Based on Sybr green PCR data, relative mRNA expression of ALP, Col-1, and Talin was significantly up-regulated in cells seeded on modified micro-scaffolds, especially the Gel:nHA = 1:1 group (**Figure 4A-C**). At 14 and 21 days of incubation, ELISA results showed that expression of ALP and Col-1 at the protein level was significantly up-regulated in cells in the Gel:nHA = 1:1 group (**Figure 4D** and **4E**). Interestingly, the cytoskeletal protein Talin was also significantly increased at 14 and 21 days, which indicates that the topological structure of nano-HA may have a positive influence on cell differentiation and migration.

In vivo experiments

Two of the original rabbits died of infection after the operation; we thus replaced them with two

more rabbits in the same group. The rabbits had a mean body weight of 3.8 ± 0.3 kg at the time of sacrifice, and no animal lost a substantial amount of weight during the study. No scaffold dislodgment was detected by x-ray in any animal. Histological analysis revealed substantially more new bone formation at 12 weeks in the Gel:nHA = 1:1 group than in the other groups (Figure 5D-F). Furthermore, the BV/TV calculated by ImageJ software was $36.1 \pm 3.6\%$ in the Gel:nHA = 1:1 group, which was significantly higher than that of the other groups (Figure 5C).

Discussion

In this study, we used degradable gelatin/nano-HA 3D micro-scaffolds as a modification to improve the bone regeneration ability of porous titanium. 3D printing techniques have allowed titanium alloy, which has been used as implant material for years, to now be individually designed with high porosity and an elastic modulus appropriate for clinical needs. Porosity can reach > 80% in scaffolds with large pores, which not only provides sufficient space for bone to grow into and facilitates an adequate supply of nutrients [18] but also alleviates the stress shielding effect in the process of bone growth [19, 20]. Thus, > 80% space can meet clinical requirements. Furthermore, the non-absorption property of titanium provides a durable mechanical advantage, avoiding the risk of mismatch between material degradation and new bone growth, which can lead to serious consequences.

However, titanium alloy is a bio-inert material that cannot provide a cell proliferation and differentiation micro-environment, especially with high-porosity and large pore size titanium. Recent modifications of porous titanium have focused on 2D modifications, such as surface acid-base chemical treatment, biological material coating, and growth factors loading, but achieving satisfactory new bone tissue volume growth into titanium scaffolds remains a challenge. Furthermore, previous studies have mainly focused on modifying of titanium with pore sizes of 200-500 μm , whereas little research has focused on modifications of large-aperture porous titanium, which is more relevant from a practical perspective [21-23]. As the diameter of a cell is only 10-20 μm , it is difficult for a cell to fill a 3D space that is 10^6 - 10^7 times larger than itself by proliferation.

In the current study, the unit cell parameters of the porous titanium were a strut width of 300 μm , average pore size of 1500 μm , and porosity of 84.8%. We used two materials, gelatin and nHA, which are generally accepted as the most important matrix components of normal human bone tissue, to construct micro-scaffolds as a strategy for porous titanium modification [24, 25]. We found that the 3D micro-scaffolds clearly accelerated osteogenesis, as exemplified by cell adhesion, proliferation, and differentiation. In particular, the Gel:nHA = 1:1 group showed the best results both in vitro and in vivo. In this group, we observed a multi-hierarchical pore structure, with a mean pore size of 156 ± 86 μm , which was closest to the structure of normal human bone. By contrast, micro-scaffolds of the Gel:nHA = 1:0 group, which were constructed of gelatin alone, had a mean pore size of 67 ± 32 μm . In these micro-scaffolds, the gelatin expanded when contacting liquid, which reduced the size of the pores, making them unsuitable for cell growth. Our novel 3D-printed hybrid scaffold system, with its multi-hierarchical pore structure and optimal pore size, appeared to create a suitable micro-environment for osteoblasts.

The extracellular matrix (ECM) plays an important role in cell survival, differentiation, and migration [26]. Talin is the key cytoplasmic protein mediating integrin adhesion to ECM; it can regulate the strength of integrin adhesion, both through affinity changes and clustering, and specifies the architecture of the adhesion site [27, 28]. We found that Talin was highly expressed in the Gel:nHA = 1:1 group. We speculate that the nHA mass can be recognized by cells, and its topological structure may have a positive influence on cell differentiation and migration, and the mechanical effects of cytoskeletal proteins. This issue warrants further exploration in the future.

This study described the successful construction of a Gel/nHA 3D micro-scaffold modification of porous titanium. The results showed that micro-scaffolds significantly enhanced cell adhesion, proliferation, and differentiation in vitro and in vivo. The Gel:nHA = 1:1 group, with its multi-hierarchical pore structure and appropriately sized nHA mass, showed the best performance. Our Gel/nHA 3D micro-scaffold titanium modification is a promising approach for the treatment of bone defects, which may

be applicable in clinical practice. Further modifications may include the addition of bioactive factors to the micro-scaffolds.

Acknowledgements

This work was supported by Youth Fund (Q2017005) of Plastic Surgery Hospital, Chinese Academy of Medical Sciences and Peking Union Medical College.

Disclosure of conflict of interest

None.

Address correspondence to: Keming Wang and Jiguang Ma, Plastic Surgery Hospital, Chinese Academy of Medical Sciences and Peking Union Medical College, No. 33, Badachu Road, Shijingshan District, Beijing 100144, China. Tel: +86-010-8555792; E-mail: wangkm_psh@163.com (KMW); majg1962@126.com (JGM)

References

- [1] Seitz H, Rieder W, Irsen S, Leukers B, Tille C. Three-dimensional printing of porous ceramic scaffolds for bone tissue engineering. *J Biomed Mater Res B Appl Biomater* 2005; 74: 782-788.
- [2] Jones AC, Arns CH, Sheppard AP, Huttmacher DW, Milthorpe BK, Knackstedt MA. Assessment of bone ingrowth into porous biomaterials using micro-ct. *Biomaterials* 2007; 28: 2491-2504.
- [3] Sen MK, Miclau T. Autologous iliac crest bone graft: should it still be the gold standard for treating nonunions? *Injury* 2007; 38 Suppl 1: S75-80.
- [4] Dimitriou R, Mataliotakis GI, Angoules AG, Kanakaris NK, Giannoudis PV. Complications following autologous bone graft harvesting from the iliac crest and using the ria: a systematic review. *Injury* 2011; 42 Suppl 2: S3-15.
- [5] Marcacci M, Kon E, Zaffagnini S, Giardino R, Rocca M, Corsi A, Benvenuti A, Bianco P, Quarto R, Martin I, Muraglia A, Cancedda R. Reconstruction of extensive long-bone defects in sheep using porous hydroxyapatite sponges. *Calcif Tissue Int* 1999; 64: 83-90.
- [6] Van der Stok J, Van Lieshout EM, El-Massoudi Y, Van Kralingen GH, Patka P. Bone substitutes in the netherlands - a systematic literature review. *Acta Biomater* 2011; 7: 739-750.
- [7] Kokubo S, Mochizuki M, Fukushima S, Ito T, Nozaki K, Iwai T, Takahashi K, Yokota S, Miyata K, Sasaki N. Long-term stability of bone tissues induced by an osteoinductive biomaterial, recombinant human bone morphogenetic protein-2 and a biodegradable carrier. *Biomaterials* 2004; 25: 1795-1803.
- [8] Nebe JB, Müller L, Lüthen F, Ewald A, Bergemann C, Conforto E, Müller FA. Osteoblast response to biomimetically altered titanium surfaces. *Acta Biomater* 2008; 4: 1985-1995.
- [9] Jonitz-Heincke A, Wieding J, Schulze C, Hansmann D, Bader R. Comparative analysis of the oxygen supply and viability of human osteoblasts in three-dimensional titanium scaffolds produced by laser-beam or electron-beam melting. *Materials* 2013; 6: 5398-5409.
- [10] Amin Yavari S, van der Stok J, Chai YC, Wauthle R, Tahmasebi Birgani Z, Habibovic P, Mulier M, Schrooten J, Weinans H, Zadpoor AA. Bone regeneration performance of surface-treated porous titanium. *Biomaterials* 2014; 35: 6172-6181.
- [11] Chai YC, Kerckhofs G, Roberts SJ, Van Bael S, Schepers E, Vleugels J, Luyten FP, Schrooten J. Ectopic bone formation by 3d porous calcium phosphate-ti6al4v hybrids produced by perfusion electrodeposition. *Biomaterials* 2012; 33: 4044-4058.
- [12] Lopez-Heredia MA, Sohler J, Gaillard C, Quillard S, Dorget M, Layrolle P. Rapid prototyped porous titanium coated with calcium phosphate as a scaffold for bone tissue engineering. *Biomaterials* 2008; 29: 2608-2615.
- [13] Yamamoto M, Hokugo A, Takahashi Y, Nakano T, Hiraoka M, Tabata Y. Combination of bmp-2-releasing gelatin/beta-tcp sponges with autologous bone marrow for bone regeneration of x-ray-irradiated rabbit ulnar defects. *Biomaterials* 2015; 56: 18-25.
- [14] Shin H, Jo S, Mikos AG. Biomimetic materials for tissue engineering. *Biomaterials* 2003; 24: 4353-4364.
- [15] Ma PX. Biomimetic materials for tissue engineering. *Adv Drug Deliv Rev* 2008; 60: 184-198.
- [16] Guo X, Gough JE, Xiao P, Liu J, Shen Z. Fabrication of nanostructured hydroxyapatite and analysis of human osteoblastic cellular response. *J Biomed Mater Res A* 2007; 82: 1022-1032.
- [17] Long M, Rack HJ. Titanium alloys in total joint replacement—a materials science perspective. *Biomaterials* 1998; 19: 1621-1639.
- [18] Li JP, Li SH, Van Blitterswijk CA, de Groot K. A novel porous ti6al4v: characterization and cell attachment. *J Biomed Mater Res A* 2005; 73: 223-233.
- [19] Niinomi M, Nakai M. Titanium-based biomaterials for preventing stress shielding between implant devices and bone. *Int J Biomater* 2011; 2011: 836587.
- [20] Ryan G, Pandit A, Apatsidis DP. Fabrication methods of porous metals for use in orthopaedic

Hybrid titanium scaffold for osteogenesis

- dic applications. *Biomaterials* 2006; 27: 2651-2670.
- [21] van der Stok J, Wang H, Amin Yavari S, Siebelt M, Sandker M, Waarsing JH, Verhaar JA, Jahr H, Zadpoor AA, Leeuwenburgh SC, Weinans H. Enhanced bone regeneration of cortical segmental bone defects using porous titanium scaffolds incorporated with colloidal gelatin gels for time- and dose-controlled delivery of dual growth factors. *Tissue Eng Part A* 2013; 19: 2605-2614.
- [22] Xue W, Krishna BV, Bandyopadhyay A, Bose S. Processing and biocompatibility evaluation of laser processed porous titanium. *Acta Biomater* 2007; 3: 1007-1018.
- [23] Otsuki B, Takemoto M, Fujibayashi S, Neo M, Kokubo T, Nakamura T. Pore throat size and connectivity determine bone and tissue ingrowth into porous implants: Three-dimensional micro-ct based structural analyses of porous bioactive titanium implants. *Biomaterials* 2006; 27: 5892-5900.
- [24] Yaylaoğlu MB, Korkusuz P, Ors U, Korkusuz F, Hasirci V. Development of a calcium phosphate-gelatin composite as a bone substitute and its use in drug release. *Biomaterials* 1999; 20: 711-719.
- [25] Chen J, Pan P, Zhang Y, Zhong S, Zhang Q. Preparation of chitosan/nano hydroxyapatite organic-inorganic hybrid microspheres for bone repair. *Colloids Surf B Biointerfaces* 2015; 134: 401-407.
- [26] Maartens AP, Brown NH. Anchors and signals: The diverse roles of integrins in development. *Curr Top Dev Biol* 2015; 112: 233-272.
- [27] Hytönen VP, Wehrle-Haller B. Mechanosensing in cell-matrix adhesions - converting tension into chemical signals. *Exp Cell Res* 2016; 343: 35-41.
- [28] Klapholz B, Brown NH. Talin - the master of integrin adhesions. *J Cell Sci* 2017; 130: 2435-2446.